Oxygen Gettering in Low-Energy Arsenic Ion Implanted Cz-Silicon

O. Oberemok[1], V. Kladko[1], V. Litovchenko[1], B. Romanyuk[1], V. Popov[1], V. Melnik[1], J. Vanhellemont[2]

[1]V. Lashkarev Institute of Semiconductor Physics NAS of Ukraine, Prospect Nauki 41, 03028 Kyiv, Ukraine

[2]Department of Solid State Sciences, Ghent University, Krijgslaan 281 S1, B-9000 Ghent, Belgium

1 Introduction

The processes for formation of the source/drain regions in metal-oxide-semiconductor field effect transistors (MOSFET) become increasingly important as device dimensions are scaled down. In order to suppress the short-channel effect, creation of an ultra-shallow junction (USJ) with high dopant activation is required [1]. In particular, low-energy implantation of As is widely used to create the n-type region. However, the formation of a high quality USJ is complicated by dopant deactivation and its accumulation near the SiO_2-Si interface [2], and by transient-enhanced diffusion (TED) as a result of the interaction of dopant atoms with intrinsic point defects [3].
Another important factor affecting the properties of the USJ in Cz Si is the presence of interstitial oxygen. It is known that oxygen precipitation in Si leads to formation of defects that act as gettering centers for metal impurities that can be responsible for increased leakage current [4, 5]. Oxygen is rapidly gettered into residual damage regions, forming stable SiO_x precipitates during annealing [6]. It was previously shown that the high-energy implanted As can influence the stoichiometry of the screen oxide [7]. A local increase of the oxygen concentration above 10^{20}cm^{-3} in the As shallow junction leads to degradation of electrical characteristics and reduction of the carrier mobility [8] by the formation of electrically inactive As-O [9] or O-As-Vacancy clusters [10]. All of these effects can lead to a degradation of the devices.
In this work, USJs were created by low-energy As^+ implantation followed by high-temperature dopant activation annealing. The redistribution of the As and oxygen atoms during the annealing were studied using Secondary Ion Mass Spectrometry (SIMS). A buried oxygen marker layer was used for a verification of the oxygen diffusion towards the As implanted region. The marker layer was created by implantation of ^{18}O oxygen isotope ions.

2 Experiment

(100) p-type 10 Ωcm Cz-Si wafers were used containing about 10^{18} cm^{-3} interstitial oxygen atoms. The samples were implanted through a 2.2 nm screen oxide with 4×10^{14} cm^{-2} As^+ ions with an energy of 5 keV. Furnace annealing of the as-implanted samples was carried out in nitrogen ambient for 0.5 to 20 minutes within the temperature range 750 °C to 950 °C. The average heating and cooling rates were 25 °C and 30 °C per second, respectively. Some of the samples were additionally ion implanted with ^{18}O (100 keV, 1.2×10^{14} cm^{-2}). Analysis of the dopant depth profiles was performed by SIMS using a Cameca IMS 4F instrument. The precise composition analysis of the thin surface layers was determined with a Time of Flight (ToF)-SIMS IV instrument by using low-energy (0.4 keV) Cs^+ ion sputtering. The depth scale was determined for each profile by measuring the crater depth with a Dektak 3030 profilometer. Peculiarities of the lattice defect creation and transformation were investigated by X-ray diffuse scattering (XDS) using a high-resolution diffractometer PANalytical XPert Pro MRD.

3 Observations

SIMS depth profiles of As and $^{60}SiO_2$ in Si before and after annealing at 950 °C for 1 and 5 minutes are shown in Fig. 1. It is seen that after annealing the implanted As is redistributed both towards the surface and into the bulk of the sample. Arsenic accumulation at the SiO_2-Si interface is increasing with annealing temperature and duration. It was also observed that the As redistribution is accompanied by changes in the oxygen concentration ($^{60}SiO_2$ intensity) in the vicinity of the USJ. In the following we call this region the Active Diffusion Region (ADR) of impurities that is located between 3 (at the SiO_2-Si interface) and 100 nm below the wafer surface. Fig. 1 shows an increase in SiO_2 signal by a factor of 3 after anneals at 950 °C for 1 minute compared to as-implanted sample. Therefore, the concentration of oxygen in the ADR clearly increases during annealing.
Annealing of the As-implanted samples leads to an increase of the screening SiO_x layer thickness and to a recovery of the surface film to the SiO_2 composition. Estimation of the oxide thickness at the 0.707 level from the maximum of the initial oxygen depth profile shows that the increase of annealing temperature leads to an increase in the screen SiO_x film thickness from 2.2 to 2.8 nm. This effect is most probably due to additional oxygen supplied from some external source. The origin of this source (annealing atmosphere or Si bulk) is not clear at the moment. Part of this redistribution of oxygen can however be attributed to oxygen gettering from the bulk of Si wafer to the As implanted region. Maxima of oxygen concentration in the ADR are reached after 1- and 3- min annealing at 950 °C and 750 °C, respectively. For longer annealing times, the oxygen concentration in the ADR decreases again and is accompanied by an increase of the surface oxide layer thickness.
The oxygen accumulation (gettering) process in the ADR happens mainly during the initial stage of thermal annealing. After that, the process of the surface oxide film growth due to absorption of oxygen from the ADR begins. In the same time intervals, the processes of implanted As redistribution and activation [2, 3] take place suggesting that both the oxygen and As redistribution are correlated. To clarify this correlation, the time dependence of As and oxygen redistribution during the annealing processes was studied more in detail.
XDS observations reveal high mechanical stresses in the As implanted region [12]. The shapes of the recorded curves indicate defects both of vacancy ($\mathbf{q}_z < 0$), and of interstitial ($\mathbf{q}_z > 0$) type, where $\mathbf{q}_z$ is the reciprocal lattice vector. The concentration of both types of defects increases after annealing at 750 °C. After annealing at 950 °C, the vacancy defects almost disappear, but the concentration of interstitial defects still increases.
In single crystal Si with lattice parameter a, ion implantation forms both tensile ($^{\Delta a}/_{a} = 7.7\times10^{-4}$) and compressive ($^{\Delta a}/_{a} = -5.64\times10^{-4}$) strained regions. Annealing leads to strain redistribution. The size of the tensile strain region is enlarged with a slight decrease in the stress after annealing at 750 °C. Simultaneously, the compressive stress is enhanced. The tensile strains disappear after annealing at 850-950 °C. At the same time, the extent of compressive strain region is enlarged with a slight decrease in the stress.
At the beginning of the 750 °C anneal, reconstruction of the implanted region occurs, and concurrently oxygen gettering from the wafer bulk takes place. The driving force for oxygen gettering in the ADR is the tensile mechanical stress gradient in the near surface region with maximum As concentration.
For anneals at 750 °C longer than 20 min, only a fraction of the As atoms is substitutional, while the rest of the As atoms is accumulated at the SiO_2-Si interface. The tensile mechanical stress in the ADR therefor decreases, and the gettered oxygen flow from the bulk diminishes. The accumulated oxygen atoms are gradually pushed to the SiO_2-Si interface. The growing SiO_2 layer can generate Si interstitials and at the same time also a reorganization of the end of range interstitials into extended lattice defects takes place.
For annealing at 950 °C, the above mentioned processes occur so quickly that separation of them is no longer possible. Even after half a minute annealing, one can already observe the three processes: arsenic segregation, accumulation of oxygen in the ADR, and an increase of the SiO_2 thickness. The reason for this is that after 5 minutes of annealing at 950 °C the processes of oxygen accumulation and growth of the SiO_2 surface layer are almost completed, and only As diffusion takes place during further anneal.
One can assume that the bulk of the Si wafer is the main source of oxygen to explain the observed oxide layer growth. In this case, the shallow-implanted As acts as a getter layer for the oxygen in the bulk of the wafer. To confirm this idea, an ^{18}O marker layer was introduced at a depth of 0.3 μm from the sample surface. This buried layer will act as an oxygen source during the annealing. It is necessary to use ^{18}O isotope to be able to separate the implanted oxygen from the background ^{16}O oxygen that is always present in Cz wafers. Fig. 2 shows SIMS depth profiles of the implanted ^{18}O atoms before and after annealing at the temperature 950 °C for 5 minutes in the As-implanted Si. The projected range of oxygen was close to 300 nm. It is seen that the implanted ^{18}O is strongly redistributed towards the As-implanted surface and is being incorporated also into the screen oxide layer on the wafer surface. In the presence of a marker layer the thickness of the screen oxide layer is increased by about 0.5 nm after the annealing.

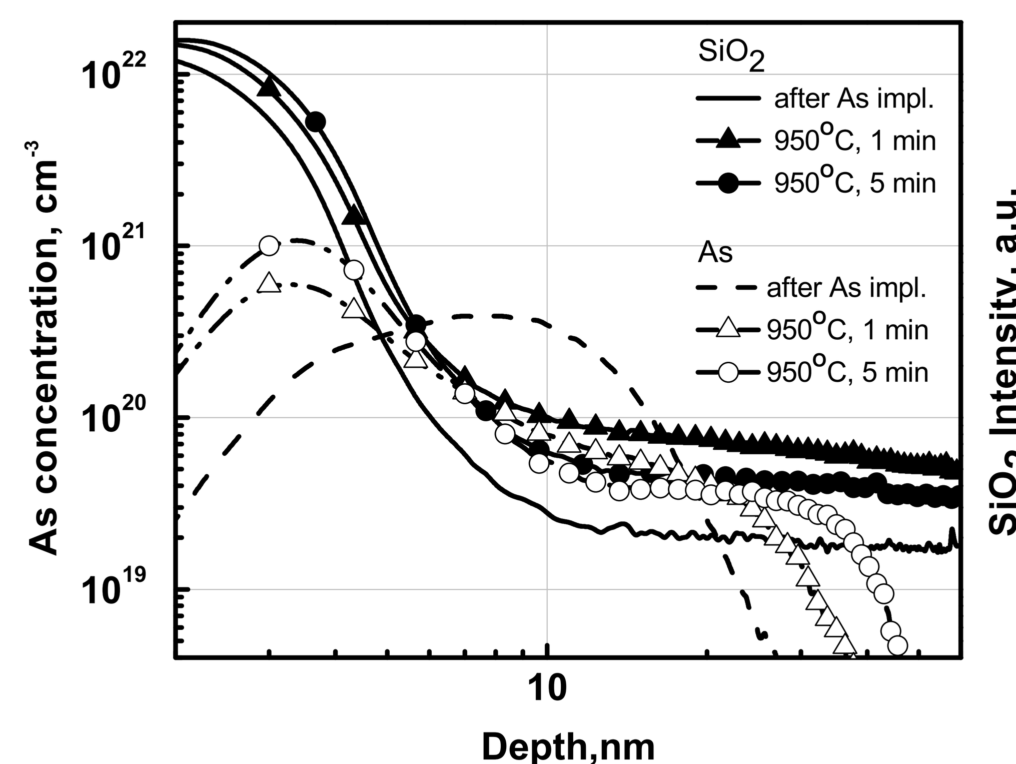

Figure 1: SIMS depth profiles of As and $^{60}SiO_2$ distributions at 950 °C annealing temperature (1 and 5 min.).

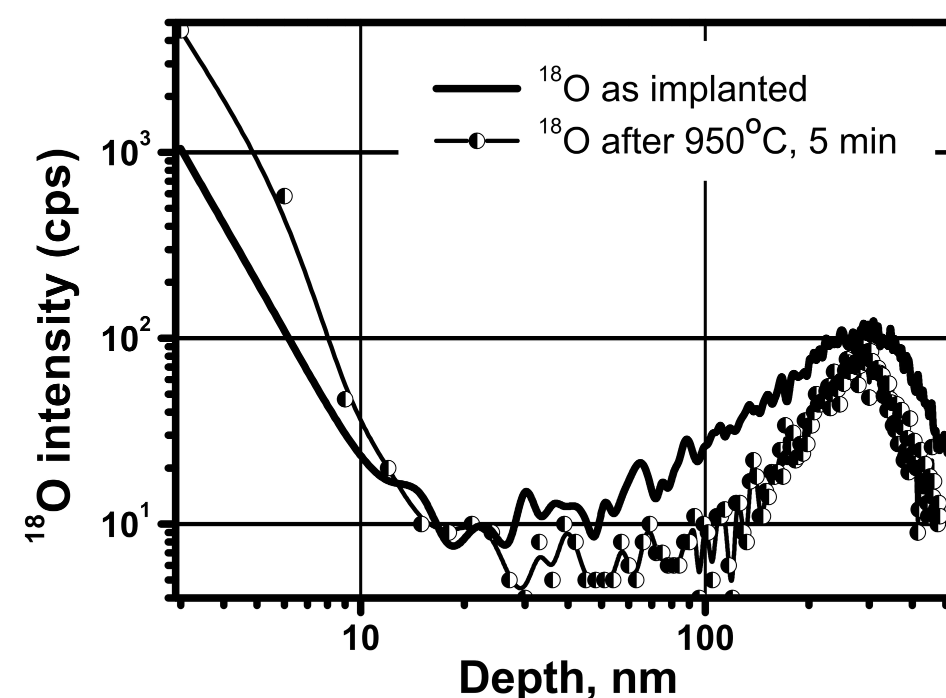

Figure 2: SIMS ^{18}O depth profiles for samples: implanted by $^{75}As^+$ and $^{18}O^+$ before and after annealing at 950 °C, 5 min.

4 Discussion

Implanted impurity redistribution occurs towards the screen oxide-Si interface. Therefore, the dopant redistribution processes in this region are examined more in detail. Comparison of the $^{60}SiO_2$ signal depth profiles for the annealed samples reveals a significant broadening of the $^{28}Si^{16}O_2$ oxide thickness for the ^{18}O implanted sample. So, the increase of surface oxide thickness occurs not only due to the gettering of ^{18}O but also due to additional ^{16}O atoms out-diffusing from the bulk of the wafer. This may be due to the following two reasons: enhancement of the gettering of the background oxygen as a result of only the ^{18}O implantation or as a result of co-implantation of $^{18}(H_2^{16}O)^+$ ions. Co-implantation of monatomic and polyatomic ions can occur due to the low mass resolution of the implanter device. Further more, the implantation of the oxygen marker layer changes the distribution of mechanical stress near the wafer surface, and this affects also the oxygen diffusion coefficient. Summarizing, the USJ formation after low-energy ion implantation is followed by an increase of the oxygen concentration in the As distribution region.
With annealing temperature increasing from 750 °C up to 950 °C, the accumulated oxygen concentration in the As distribution region decreases accompanied by an increase of the oxide thickness. Increasing the annealing time also increases the thickness of the surface oxide. Our model experiments clearly show that during thermal annealing, implanted ^{18}O diffuses from the depth of ≈300 nm towards the surface and accumulates at the Si-SiO_2 interface region clearly indicating the oxygen gettering effect.
The appearance of concentration peaks in the $^{60}SiO_2$- signal is due to the presence of SiO_2 precipitates in the As-rich region. The variation of the intensities of these peaks as function of the anneal temperature can be explained as follows. The critical radius for the formation of SiO_2 precipitate depends not only on the supersaturation of interstitial oxygen but also on the supersaturation of intrinsic point defects as described by [13]

$$R_{cr} = \frac{2\sigma\Omega}{kTln\frac{C}{C_{eq}}(\frac{V}{V_{eq}})^{\beta}(\frac{I}{I_{eq}})^{-\gamma}}. \quad (1)$$

σ (≈ 0.43 J/m^2 for SiO_2) is the interface energy [14]. Ω (= 2.25×10^{-29} m^3 for SiO_2) is the volume per oxygen atom in the precipitated SiO_x phase [15]. k is the Boltzmann constant and T the temperature. C, V, and I are the concentrations of interstitial oxygen, vacancies, and self-interstitials, respectively. C_{eq}, V_{eq}, and I_{eq} are their equilibrium concentrations, respectively [13, 16]. β and γ are the number of vacancies and interstitials, respectively, absorbed in the precipitate per precipitated oxygen atom. The formation energies of the intrinsic point defects depend on the Fermi level and also to the stress introduced by the substitutional dopant atoms and the precipitate [17, 18].
As follows from Eq. (1), a vacancy supersaturation leads to enhanced precipitation due to a decrease of the critical radius R_{cr}. The higher vacancy supersaturation at 750 °C due to the lower vacancy solubility V_{eq} combined with the higher supersaturation of oxygen, can explain the higher intensity of the $^{60}SiO_2$ signal peak compared to that at 950 °C. Another reason may be a higher rate of activation of implanted As at 950 °C leading to a decrease of the vacancy supersaturation. In addition, the oxygen concentration driven into the region of As redistribution is higher at 750 °C which, together with smaller oxygen solubility, leads to a higher oxygen supersaturation and an additional decrease of the critical radius for SiO_x precipitate nucleation.
The decrease in the intensity of the $^{60}SiO_2$ signal after longer annealing times may be attributed to the dissolution of SiO_x precipitates due to energetically more favorable oxidation at a surface SiO_2 layer as well as due to the possible increase of the concentration of Si self-interstitials produced by such oxidation, which according to Eq. (1) leads to an increase of the critical radius for precipitate nucleation. At the initial stage of annealing, after rapid recombination of part of the implantation induced intrinsic point defects, the As atoms are dominantly in metastable interstitial positions, creating a tensile stressed near surface layer, which enhances oxygen gettering from the wafer bulk to the heavily As doped near surface layer during the anneal. At 750 °C, this process goes on for about 3 to 6 minutes. Longer annealing leads to activation of part of the As atoms whereby they become substitutional and thus remove vacancies, while the other part of the As atoms is accumulated at the SiO_2-Si interface after rapid diffusion of interstitial As atoms. The tensile stress therefor decrease, the enhanced oxygen flow from the bulk is terminated, and oxygen diffuses gradually from the ADR to the Si-SiO_2 interface, increasing the thickness of the surface oxide. At higher annealing temperatures (950 °C), these processes of restructuring of the surface layer, oxygen gettering from the wafer bulk and oxide film growth occur over a much shorter time period (< 1 min). Further growth of the oxide surface layer occurs due to absorption of gettered oxygen for a time from 1 to 5 minutes. Further annealing at 950 °C leads to a change in the As distribution profile partly due to interaction of point defects. Oxygen atoms do not participate in these processes any more.

5 Conclusions

Point defect stimulated gettering of oxygen during thermal activation of implanted As in Si has been observed. The dependence of As and oxygen depth profiles on thermal anneal temperature and duration have been investigated. An increase of the surface oxide thickness during annealing was observed and was explained by oxygen gettering from the Si wafer bulk towards the USJ region. This effect was confirmed by a model experiment with additional implantation of $^{18}O^+$ ions into Si substrate. It was shown that implanted ^{18}O atoms are strongly redistributed towards the As-implanted surface, and are being incorporated into the surface screen oxide layer. Oxygen redistribution is related with the tensile mechanical stresses, vacancy concentration distribution (and Fermi level effect?) in implanted Si. The influence of point defects, both vacancies and interstitials, on the process of formation of impurity precipitates during formation of ultra-shallow junctions was also discussed.

References

[1] International Technology Roadmap for Semiconductors (2012).
[2] D. Kruger et al, J. Vac. Sci. Technol. 22, 455 (2004).
[3] H. Rucker et al, Appl. Phys. Lett. 82, 826 (2003).
[4] H. Shirai et al, Appl. Phys. Lett. 54, 1748 (1996).
[5] R. Falster et al, Appl. Phys. Lett. 59, 809 (1991).
[6] T. J. Magee et al, Appl. Phys. Lett. 39, 564 (1981).
[7] I. J. R. Baumvol et al, Braz. J. Phys. 24, 529 (1994).
[8] T. Hirao et al, J. Appl. Phys. 50, 5251 (1979).
[9] R. Kögler et al, Phys. Stat. Sol. (a) 113, 321 (1989).
[10] G.-H. Lu et al, Appl. Phys. Lett. 92, 211906 (2008).
[11] R. C. Newman, J. Phys.: Condens. Matter 12, R335 (2000).
[12] O. I. Gudymenko et al, Ukr. J. Phys. 53, 140 (2008).
[13] J. Vanhellemont and C. Claeys, J. Appl. Phys. 62, 3960 (1987); ibidem 71, 1073 (1992).
[14] A. Borghesi et al, J. Appl. Phys. 77, 4169 (1995).
[15] V. G. Litovchenko et al, Ukr. J. Phys. 5, 958 (2007).
[16] A. Sarikov et al, J. Electrochem. Soc. 158, H772 (2011).
[17] J. Vanhellemont et al, ECS J. Solid State Sci. Technol. 2, 166 (2013).
[18] K. Sueoka et al, J. Appl. Phys. 114, 153510 (2013).